SBUF

ID: 12903

Härdningstemperaturens effekter på den unga betongens egenskaper

Effects of curing regime on the properties of young concrete

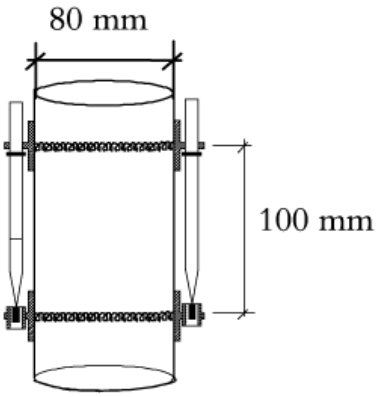

Andrzej Cwirzen, Katalin Orosz

2016-11-11

PREFACE

The present project was carried out as further development of a former Nordic research project - Crack-Free-Con.

Laboratory experiments of the project were implemented at Luleå University of Technology. The measuring equipment was adapted and modified according to the project needs. The majority of the work was done by a PhD candidate Katalin Orosz with support from the TestLab staff. The report was prepared jointly by Katalin Orosz and Andrzej Cwirzen who was the main supervisor in the last stages of the project. The co-supervisor was Prof. Hans Hedlund who also represented Skanska as the main SBUF applicant for that project.

SHORT SUMMARY

The “Effects of curing regime on properties of young concrete” financed by the SBUF/TRV has aimed to verify in the laboratory the effects of varying curing temperatures on autogenous shrinkage and self-desiccation of selected concrete mix formulations, with the intention to provide bases for updated models in order to quantify and predict early-age cracking risk under variable temperature curing conditions.

Shrinkage tests were performed on ordinary Portland cement based concretes exposed to variable curing temperatures. The collected data consisted of the free deformation, the temperature of the controlling water bath, the temperature in the center of the samples, and the room temperature. The recorded free deformation has been split into autogenous and thermal deformation by means of the existing maturity concept-based model from Hedlund (2000).

The study showed that existing models have certain drawbacks mostly related to a possible swelling which is not accounted for. That phenomenon becomes increasingly important for new generation of blended Portland cements and when secondary cementitious binders are used.

The results obtained within this project have clarified problems of current models and as such it is an excellent foundation for more detailed future research leading to the development of new more reliable models. One new aspect which should be studied in depth is a possibility to utilize the observed swelling to decrease cracking risk of young concrete. If that swelling would be introduced in a controlled manner for example by a proper concrete mix design or optimized curing it could decrease shrinkage and thus cracking risk of young concretes when the tensile strength is relatively low.

Successful implementation of that approach would lead to development of improved “crack free” concrete. It would alter the production processes, concreting technology and would improve quality of hardened concrete. Lower crack risk would also enhance the sustainability of that material and decrease early age repair costs.

KORT SAMMANFATTNING

¨Forskningsprojektet ” Härdningstemperaturens effekter på den unga betongens egenskaper” som finansieras av SBUF/TRV har syftat till laboratorieverifiering av härdningstemperaturens effekter på autogen krympning för ett urval av betongsammansättningar, med avsikten att ge baser för uppdaterade modeller för att kvantifiera och förutsäga tidig ålder sprickbildning risk under varierande temperaturhärdningsbetingelser.

Krympningstester utfördes på Portland cementbaserade betong som utsätts för varierande härdningstemperaturer. Insamlade data bestod av den fria deformation, temperaturen på den styrande vattenbadet, temperaturen i mitten av proverna, och rumstemperaturen. Den inspelade fri deformation har delats upp i autogen och termisk deformation med hjälp av befintliga mognadskonceptbaserade modell från Hedlund (2000).

Studien visade att befintliga modeller har vissa nackdelar, främst relaterade till en eventuell svällning som inte beaktas. Fenomenet blir allt viktigare för en ny generation av sammansatta portlandcement och i de fall då sekundära cementbaserade bindemedel används.

Resultaten från denna studie klarlägger problemen hos de nuvarande modellerna och utgör en utmärkt grund för mer ingående framtida forskning för att utveckla nya och mer tillförlitliga modeller. En ny aspekt som bör studeras mer är möjligheten att utnyttja den observerade svällningen för att minska sprickrisken i den unga betongen. Om denna svällning kan introduceras på ett kontrollerat sätt genom till exempel ett väl anpassat betongrecept eller optimerade härdningsförhållanden kan eventuellt krympningen och därmed sprickrisken minskas för unga betonger med relativt låg draghållfasthet.

Ett framgångsrikt genomförande av en sådan studie skulle kunna leda till utveckling av förbättrade ”sprickfria” betonger. Vidare har den potentialen att förändra tillverkningsprocessen och gjutteknologin, samtidigt som egenskaperna i den hårdnade betongen förbättras. En lägre sprickrisk skulle även öka hållbarheten för materialet och minska kostnaderna för tidiga reparationer.

CONTENT

1 INTRODUCTION

In concrete technology, the importance of the curing temperature (McDaniel, 1915; Davis et al, 1933) as well as moisture state (Powers, 1948) has been well known to describe the hardening process. The first model presented (McIntosh, 1949) only considered the impact of the (maximum) concrete temperature on strength development. The author used a basic maturation index, defined by the accumulated area under the concrete temperature-time curve down to a selected reference temperature, which is the basic parameter related to the concrete strength growth.

The approach has been quickly adopted by the Nordic countries as a rational and simple way to analyze the hardening of concrete at varying temperatures, and in particular for winter casting, while taking into account the temperature and the age of the concrete. The maturity concept for the concrete hardening has been presented in the 1950s and was refined later by Freiesleben et al. (1977) and Byfors (1980). The so-called Arrhenius equation was used to describe the dependence between curing process and concrete temperature development. This concept has been used worldwide for the past 40 years. Models have proven to be suitable to describe the free deformations (the sum of autogenous shrinkage and thermal dilation) for concretes with w/c ratios around 0.40 using "moderate heat" cement, Hedlund (2000). Unfortunately, there is still a need to develop universal maturity function valid for various types of modern cements and concretes which often incorporate secondary cementitious binders such as fly ash or blast furnace slag. Difficulties have arisen in low w/c, "high heat" cement mixers, or concrete subject to complex temperature variations, e.g., Fjellström (2013), Orosz at al. (2014).

The ability to reliably predict properties of young concretes especially, strength development, shrinkage and swelling are fundamental to create models estimating risk of cracking. These models are crucial for the contractors to properly implement curing and after-treatments of young concretes and to avoid financial losses caused by extensive cracking

Purpose and goal

The aims of the current project can be listed as:

- to study the effects varying curing temperature on autogenous shrinkage and self-desiccation shrinkage
- to create basis for models to describe and predict autogenous shrinkage

2 LITERATURE REVIEW

2.1 Autogenous shrinkage and cracking risk

The young concrete is at an increased risk of cracking due to the combination effect of differential shrinkage and internal restraints. In mass concrete, differential shrinkage results from that the heat generated within the body of the structure cannot be dissipated quickly, resulting in larger temperature gradients and corresponding larger autogenous shrinkage (AS) in the center, while the aggregates act as restraint; Lura (2003). In thin structures with large surfaces drying out, combined autogenous and drying shrinkage can generate high enough stresses that lead to early age cracking.

Autogenous shrinkage, or self-desiccation shrinkage are an inherent part of the total deformation that is unavoidable; Persson (1997), Jensen et al. (2001), Tazawa et al (2000). Autogenous shrinkage is a direct consequence of chemical shrinkage occurring after the final set of concrete, Tazawa et al. (2000), Jensen et al. (1999), Lura et al. (2003), Holt (2001), Kovler et al. (2006). With the recent increased use of high early strength-, high performance-, and/or blended binder concretes, with low water/cement ratio the AS make up for a substantially larger part of the total shrinkage, significant enough to possibly induce micro- or macro cracking due to the increased paste volume and higher binder content per unit volume; Cusson et al. (2008), Bjøntegaard (1999), Hedlund and Jonasson (2000), Turcry et al. (2002). In a high performance concrete sample, autogenous shrinkage reached a value of 250 x 10^{-6} strains by 24 hours of age, presenting a significant cracking risk if movements are restrained; Cusson et al. (2008).

Typically, the autogenous deformation (AD) manifests as shrinkage. However, the recent results reported on cases where a substantial autogenous expansion or "AD swelling", as commonly referred to, has occurred; Tazawa et al. (2000). This expansion can be beneficial for concrete, since it has the potential to partially mitigate tensile stresses when the concrete has a very low modulus of elasticity. It was recommended to use the net shrinkage value, which occurs after early-age expansion, for estimating cracking risk in young concrete undergoing early expansion, Cusson et al. (2008). That approach ignores the possible shrinkage-mitigating effects of the early-age expansion.

2.2 Decoupling autogenous and thermal deformation

During hydration, if the inherent hydration-induced temperature changes of the concrete are not controlled, after setting, autogenous deformation (AD) and thermal deformation (TD) occur simultaneously and can be estimated using equations 1.1 and 1.2.

$$\varepsilon_{tot} = \varepsilon_{AD} + \varepsilon_{TD} \qquad (1.1)$$

$$\varepsilon_{TD} = \alpha \cdot \Delta T \qquad (1.2)$$

Where ε_{tot} is the total deformation, ε_{TD} is the thermal dilation, ε_{AD} is the autogenous deformation, αT is the coefficient of thermal expansion (CTE) and ΔT is the temperature change.

The total deformation (AD + TD) can be measured in the laboratory. However, separating the two effects is necessary in order to determine the relative importance of each mechanism separately. For a generalized model capable to describe any conceivable temperature history and to calculate shrinkage-induced stresses, it is fundamental to have a robust, generalized model for both AD and TD; see Bjøntegaard (1999).

There is no clear agreement in literature whether the maturity concept can be applied to describe AD development under variable temperature curing conditions. It was suggested by Hedlund and Jonasson (2000) that the maturity concept based on the effective age could be used by expanding it with a temperature-correcting factor. Some researchers, e.g., Turcry et al. (2002) reported that it is possible to separate AD and TD in cement pastes, based on the maturity concept, by offsetting the total deformation by thermal deformation part as long as the temperature range is between 10^0C and 40^0C. In contrast, other reports by e.g., Jensen et al. (1999), and Bjøntegaard (1999) indicated that the maturity concept is unsuitable. It has been well known and implemented in early models that the magnitude of AS depends on the maximum temperature reached throughout the curing process; Emborg (1989), and Hedlund (2000). Recent research revealed that different imposed temperature paths (histories) result in different AD developments, even despite the same degree of hydration.

Measuring AD directly, at constant temperature levels, and deducing AD from these for other temperature levels is not possible due to both the magnitude and development rate of AD showing strong temperature history dependence; e.g., Jensen et al. (1999), Bjøntegaard (1999), Bjøntegaard and Sellevold (2001), and Klausen (2016). In it has been shown that AD obtained from isothermal tests, in the opposite to concretes subjected to realistic (field) temperature development is fundamentally different. That includes also the early-age autogenous swelling developing in the cooling down phase, which then slowly turns into contraction again; Bjøntegaard (1999), Bjøntegaard and Sellevold (2001). Furthermore, the behavior has been found to be unsystematic, even when assuming a range of "realistic" coefficients of thermal expansion (CTE). Another report supports the unsystematic behavior, emphasizing that a higher temperature does not necessarily lead to a higher AS. As a result, AD in a real structure cannot be predicted from isothermal test results because the fundamental behavior (contraction or expansion) depends on the specific imposed temperature history. Thus this indicates that AD depends on more than hydration degree, e.g., Lura et al. (2001).

Other, non-maturity concept-based approaches include a method based on time-temperature dependent activation energy, Chu et al. (2012) or relating AS to negative capillary pressure in the pore system during early ages, Grondin et al. (2010).

2.3 Thermal dilation

Assuming that the development of CTE over time is known for the young concrete, the total deformation could be split into AD and TD. Unfortunately, the CTE- time relation is highly nonlinear and depends on the moisture content; Sellevold and Bjøntegaard (2006). It has been shown by Viviani et al. (2007) that the development of CTE appears to be less affected by the

curing regime history than the AD and may also be influenced be the pore structure, Grasley and Lange (2007). After casting, the CTE decreases sharply during the first hours due to large amount of unbound water (above $20x10^{-6}$/°C), as observed by Chu et al. (2012), Cusson and Hogeveen (2006), and Loser et al. (2010) to a minimum value around setting time (~7x10-6/°C), and thereafter it slowly increases with time due to self-desiccation, Sellevold and Bjøntegaard (2006), converging to the value characteristic of hardened concrete (9…12 x10-6/°C). The reduction around setting time is due to the fact that before setting, the free water is continuous while as a solid skeleton builds up the continuity is disrupted.

Ranges of CTE (typically for hardened concrete) are available in literature, but data for early-age concrete are rather limited. It is possible to measure CTE at certain time intervals with a setup and steering detailed in [10] with tests steered by applying the temperature load stepwise. During the intervals where the temperature is kept constant, the deformation is purely autogenous. It is important to underline that the AD developed up to that point is still not "absolute", as it is a function of the entire proceeding temperature history. Conversely, when an "instantaneous" thermal load (in steps) is applied, ideally, pure TD can be measured. A similar method was applied for mortars by Loukili et al. (2000) and pastes by Turcry et al. (2002) and Maruyama and Teramoto (2013), where CTE was measured stepwise, and then interpolated.

2.4 Autogenous swelling

The current state-of-the-art on AD swelling is scarce and conflicting. While bearing in mind that it is not necessarily possible to predict the AD behavior of the concrete based on the paste behavior, since the filler and fine aggregates in concrete influence early hydration according to Sellevold et al. (2005), a brief survey on the phenomenon of observed AD swelling is given. Autogenous expansion in early age concrete/mortar typically takes place after the cooling off stage when exposed to variable temperatures. It was shown in Bjøntegaard (1999) that if curing temperatures reach or exceed 50^0C, the natural cooling down phase was characterized by a reduced rate of AS followed by autogenous expansion in concrete. The process started at approximately 4 days of age. The observed expansion was related to thermally induced swelling. Heating-cooling curing regime has been observed to cause AD swelling during the cooling off phase, lasting until the temperature levels off in Viviani et al. (2007). The AD swelling is likely to appear for w/c ratios over 0.40. Recently, slow expansion of over 10 days was observed in fly ash concretes; Klausen (2016). The onset of swelling about coincides with the maximum temperature and continues throughout the cooling down phase. Swelling is prominent when $\Delta T \leq 20$°C, regardless of fly ash content (17...45%). The Type I OPC reference (ANL Ref), however, exhibits swelling despite that it has undergone a 30°C temperature change. AD swelling in OPC concrete with 50% fly ash (Fig. 5), w/c 0.30, under 20°C isothermal conditions has been reported by Termkhajornkit et al. (2005). The expansion happens well after the concrete has cooled down; the temperature in the sample did not reach 25°C at any point. The swelling is prominent around day five, lasting for 7-8 days afterward. The authors attribute the swelling to possible ettringite formation in large amounts. No swelling was observed in mixes with only 25% fly ash. Maruyama and Teramoto (2011) observed marked (back-calculated) AD swelling in both OPC cement paste and OPC with 30% and 45% blast furnace slag (w/c 0.40) with a maximum temperature of 60°C, starting around 50 hours, early into the cooling down phase (~50°C), and lasting for the entire duration of the cooling down phase.

A smaller but steady swelling was observed in the OPC sample cured at 40°C. AD swelling has been also linked to possible ettringite formation in mixes made with coarser cements by Bentz et al. (2001).

3 EXPERIMENTAL PROCEDURE

3.1 Materials

Tests were performed on ordinary concrete with two w/c ratios of 0.38 and 0.55. Concrete mix designs are shown in Table 1.

Two types of Portland cements were used: BAS cement and ANL (Anläggningscement Slite). The ANL cement series is not complete; ANL cement has been used only for control mixes after unexpected initial BAS results. Therefore, a regular w/c 0.55 ANL mix, and a "home" mix denoted as ANLFA, made by replacing 30% of the binder by fly ash have been mixed. In the ANLFA mix, all the 16/27 aggregate has also been replaced by 8/16 due to the test specimen diameter:d_{max} ratio (80:27 vs. 80:16) possibly skewing the results.

Cement properties are shown in Table 2. The BAS cement is Type II/A-V 52.5N cement containing 16% fly ash and 4% limestone and is produced by Cementa Ltd. in Sweden. The ANL cement is CEM I 42,5 N - SR 3 MH/LA low C_3A cement with lower fineness designed especially for massive structures.

Table 1. Concrete mix designs used in the project; BAS and ANL 0.55 recipes provided by Cementa

	BAS 0.38		BAS 0.55		ANLFA 0.38		ANL 0.55	
	kg/m^3	L/m^3	kg/m^3	kg/m^3		kg/m^3	L/m^3	kg/m^3
cement	470	157	360	120	294	91.7	340	106
Fly ash					126			
0/8	975	361	1067	395	928	343	1072	397
8/16	790	298	733	277	844	318	398	150
16/27							401	150
water, eff.	179	179	198	198	168	168	187	187
air content		5		10		5		10

Table 2. Physical and chemical properties of binder

Property	BAS cement	ANL cement
Blaine-fineness	450 m^2/kg	310 m^2/kg
Setting time	150 min	160 min
Compact density	3000 kg/m^3	3200 kg/m^3
CaO	55.4%	64.1%
SiO_2	24.0%	22.4%
Al_2O_3	6.7%	3.7%
Fe_2O_3	N/A	4.5%
MgO	2.8%	1.2-1.5%
K_2O	1.3%	N/A
SO_3	3.4%	2.4%
Water-soluble Cr^{6+}	< 2 ppm	< 2 ppm

C_3A	5.2%	2.1
C_3S	N/A	48%
C_2S	N/A	28%
C4AF	N/A	13.8%

3.2 Test set-up

The used measuring test set-up was based on earlier work done at LTU by Hedlund (2000) and Fjellström (2013). In that setup the free deformation is measured on Ø=80mm, h=300mm concrete cylinders by two strain gauges of type LVDT Schaevitz type 010 MRH, mounted on composite bars made of carbon. The gauges are symmetrically mounted on the two opposing sides of the cylinder, held in position by a pair of coils (Figure 1). A thermocouple is cast in the center of the cylinder.

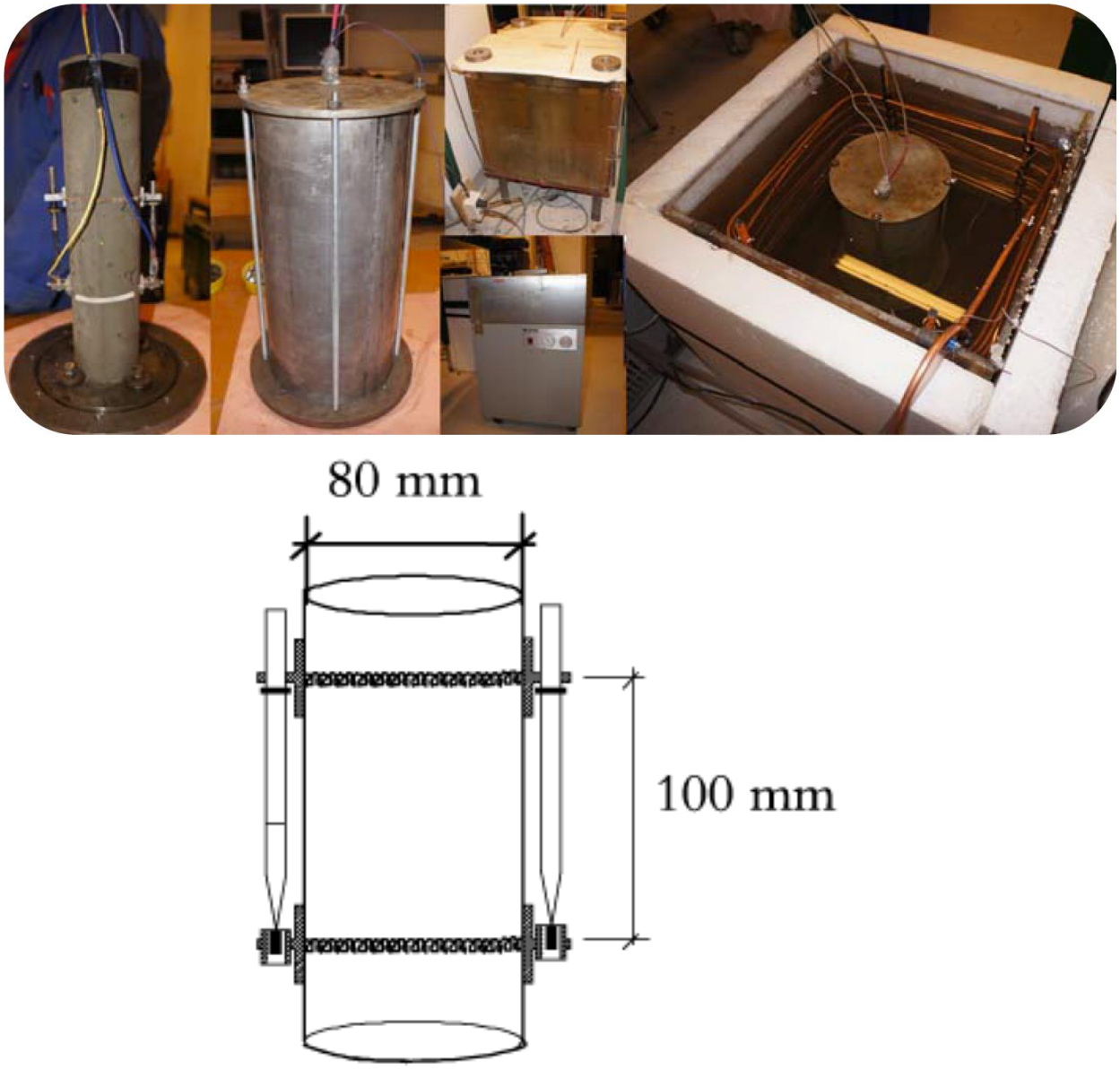

Fig. 1. Measuring setup to be used for free deformations

For every (variable) temperature history/material combination, two specimens were cast; a heat-cured and a reference (20^0C isothermal) sample. The temperature of the specimens was controlled by the temperature in the water tank with ± 3^0C accuracy. The used curing regimes are shown in Figure 2. They consisted of the initial adiabatic rise, constant curing temperature (6^0C, 35^0C and 50^0C) which simulated the heat curing and cold water casting. The constant temperature was kept for 1, 3 and 5 days. In the last stage constant cooling rate was applied followed by a steady temperature of 20^0C.

The adiabatic rise was calculated using ConTest Pro software, which enables to calculate temperature developments and cracking risk in hardening concrete. The steering for the cooled down sample has been inverted so that the rate of cooling down/heating up to 20^0C occur at the same rate as for the heat-cured samples. The total duration of all tests was 14 days.

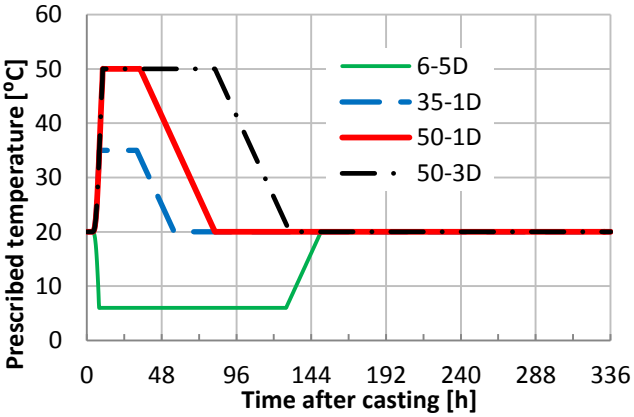

Fig. 2. Curing temperature profiles

Specimens were allowed to develop their natural adiabatic temperature rise until the mounting of the linear variable transducers, which was done approximately 8h after casting. The water bath was heat up along the same adiabatic temperature path to enable later placement of specimens with installed transducers without a thermal shock. The samples were lowered into the bath in a metal encasing which ensured perfect sealing against moisture. All measurements started at 8.5 hours after casting.

The collected data consisted of:

- free deformation,
- the temperature of the controlling water bath
- the temperature in the center of the samples
- the room temperature.

4 EXPERIMENTAL RESULTS AND DISCUSSION

4.1 Compressive strength

The obtained compressive strength values are show in Figure 3 and Figure 3-1. The 28-days compressive strength was the highest for mix BAS 0.38 and the lowest for BAS 0.55. This can be directly related to the decreased water to cement ratio. Two mixes produced using ANL cement showed a lower strength of around 50 MPa, which can be directly related to a lower specific surface area. Compressive strength development for concretes produced with BAS cement is shown in Figure 4. Higher W/C ratio resulted in a generally lower compressive strength values. Curing at higher temperatures resulted in higher early age strengths. The long term strengths were lower for heat cured samples.

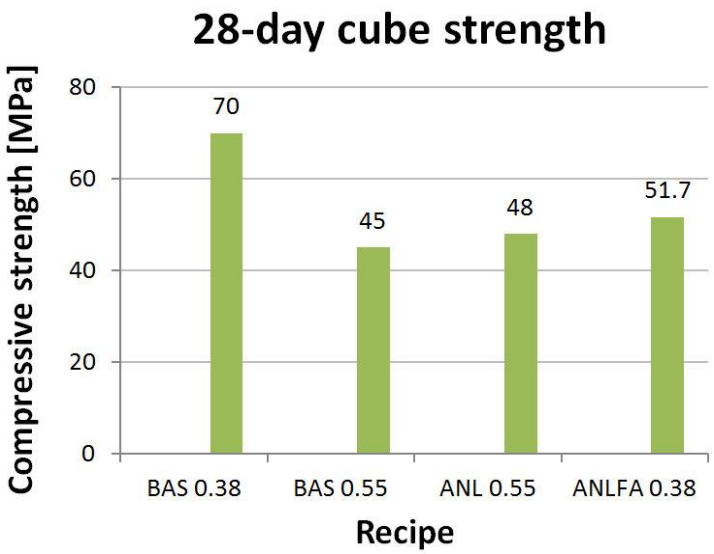

Fig 3. 28-day compressive strength values

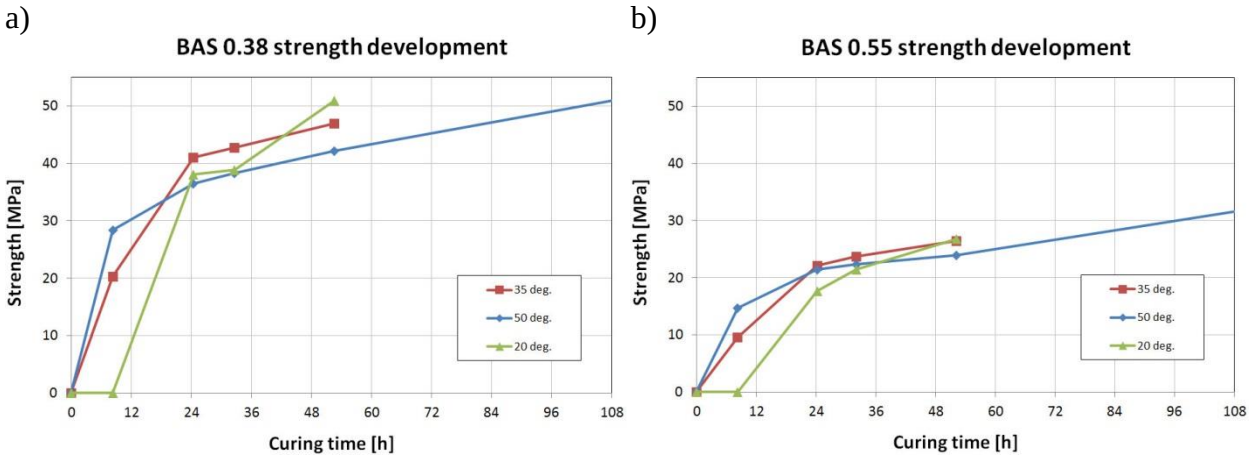

Fig. 4. Development of compressive strength of concrete produced with BAS cement and having w/c ratio of (a) 0.38 and (b) 0.55

4.2 Free deformations

The measured deformations for various curing regimens are shown in Figures 5-6 for BAS and ANL cement respectively (Figure 7). Negative values represent shrinkage, while positive values expansion (including AD swelling and/or thermal expansion). Free deformation measurements started at 8.5 h after casting (zero time). For the heat-cured w/c 0.38 samples, all deformation plots begin with an initial expansion. The thermal peak for the sample cured at 35^0C is lower than for the one cured at 50^0C samples. In general for all curing regimes a rapid shrinkage was observed at constant temperature plateau (1 or 3 days). All samples showed expansion during heating-up phase. However, in the case of samples shown in Figure 4a where curing began with cooling down to 6 degrees a shrinkage was measured followed by a short period of expansion and finally by shrinkage during curing at constant 6 degrees. Specimens showed expansion during the heating-up phase from 6 degrees to 20 degrees. Similar pattern was observed for the remaining 3 specimens but in reverse order. It can be summarized that the cooling down phase always caused shrinkage followed by short period of expansion.

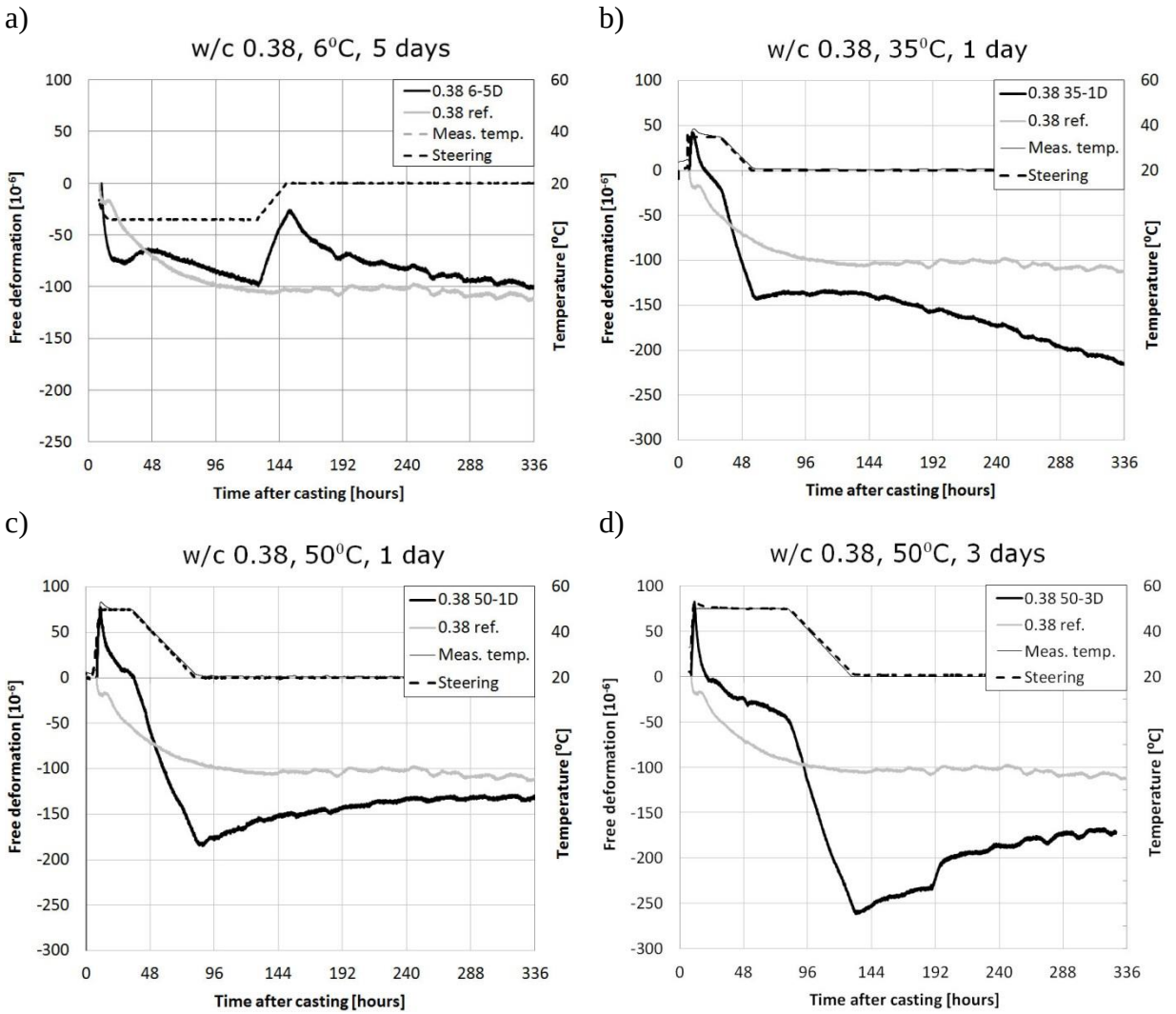

Fig. 5. Individual free deformation plots for w/c 0.38 recipes with BAS cement.

An interesting observation was a higher shrinkage rate of sample subjected to cooling to 6 degrees (Fig 4a) in comparison with the isothermally cured reference sample. The reason behind that

behavior cannot be explained based on the obtained data. Presumably additional contribution from hydration processes should be considered and investigated in the future. The same sample showed ultimate shrinkage measured after 336 hours to be very close to the isothermally cured reference sample. It is possible that after longer time a cross-over effect could occur indicating that low temperature curing (simulating cold weather casting) could hinder shrinkage only temporarily at the early stage. This phenomenon could lower cracking risk due to autogenous shrinkage at the early age when the developed tensile strength of binder matrix is very low.

The observed during the forced cooling phase shrinkage is a combination of autogenous shrinkage and thermal contraction. The measured values are not directly proportional to the actual temperature drops, which indicate that the thermal expansion (or contraction) coefficient is time and temperature dependent, Table 3. It is important to emphasize that during the cooling off stages, autogenous shrinkage and thermal deformation occur simultaneously. At earlier stage, during hydration the autogenous shrinkage will dominate except when curing started with forced cooling don phase. Table 3 summarizes the measured contraction (shrinkage and thermal dilation).

Table 3. Thermal contraction during cooling down phase in w/c 0.38 samples

Contraction [μstrain]	ΔT [^{0}C]	Occurrence; length [h]
-45	+14^{0}C (6→20^{0}C)	126-149 [23]
37	-15^{0}C (35→20^{0}C)	29-53 [24]
180	-30^{0}C (50→20^{0}C)	32-80 [48]
210	-30^{0}C (50→20^{0}C)	80-132 [48]

When comparing the two 50^{0}C levels, the thermal drop belonging to the same ΔT, but with a two-day offset, increases from 180 to 210 microstrains. This may suggest that the CTE(t) is noticeably increasing during these 2 days. Alternatively, it may imply that these two distinct curing paths result in a noticeably different concrete with a different CTE. Furthermore, a ~45 micro strain expansion during ~1 day can be seen for the sample cured following 5-6D procedure while allowed to warm up to room temperature again. This sample had presumably delayed hydration, while the 50-3D accelerated hydration. At about the same time after casting, the 50-3D sample exhibits a nearly five times larger contraction during cool-off period, which complies with earlier observations by Sellevold and Bjøntegaard (2006). The CTE gradually increases from a minimum value at around the setting time, slowly converging to the value characteristic of hardened concrete.

Delayed expansion can be observed in the 50^{0}C samples after the cooling down phase and stabilization of the temperature at 20^{0}C. Based on the obtained data it is impossible to determine time when the autogenous expansion started. It can, however, be clearly seen that expansion is measured when the temperatures are constant (20^{0}C) which excludes the thermal expansion/swelling component. Hence, the swelling seen, starting at the 130 hour mark (0.38 50-3D) and at 82 hours (0.38 50-1D) is most probably the autogenous deformation.

The measured deformations for samples produced with w/c ratio of 0.55 from BAS cement and exposed to the same curing regimes (Figure 2) are shown in Figure 5. All observed trends are

similar as in the case of w/c ratio of 0.38; however, the ultimate maximum deformation values appeared to be 10-20% higher. It is most probably caused by the combined effects of thermal expansion and autogenous shrinkage. Higher w/c ratio increased porosity and altered the chemical composition of the hardened cementitious binder matrix when comparing the same time-intervals counted from the time of mixing. Both factors have a direct effect on the extent of thermal expansion and autogenous shrinkage. In order to verify the actual contribution of both types of deformations to the ultimate measured values, a more detailed study should be made.

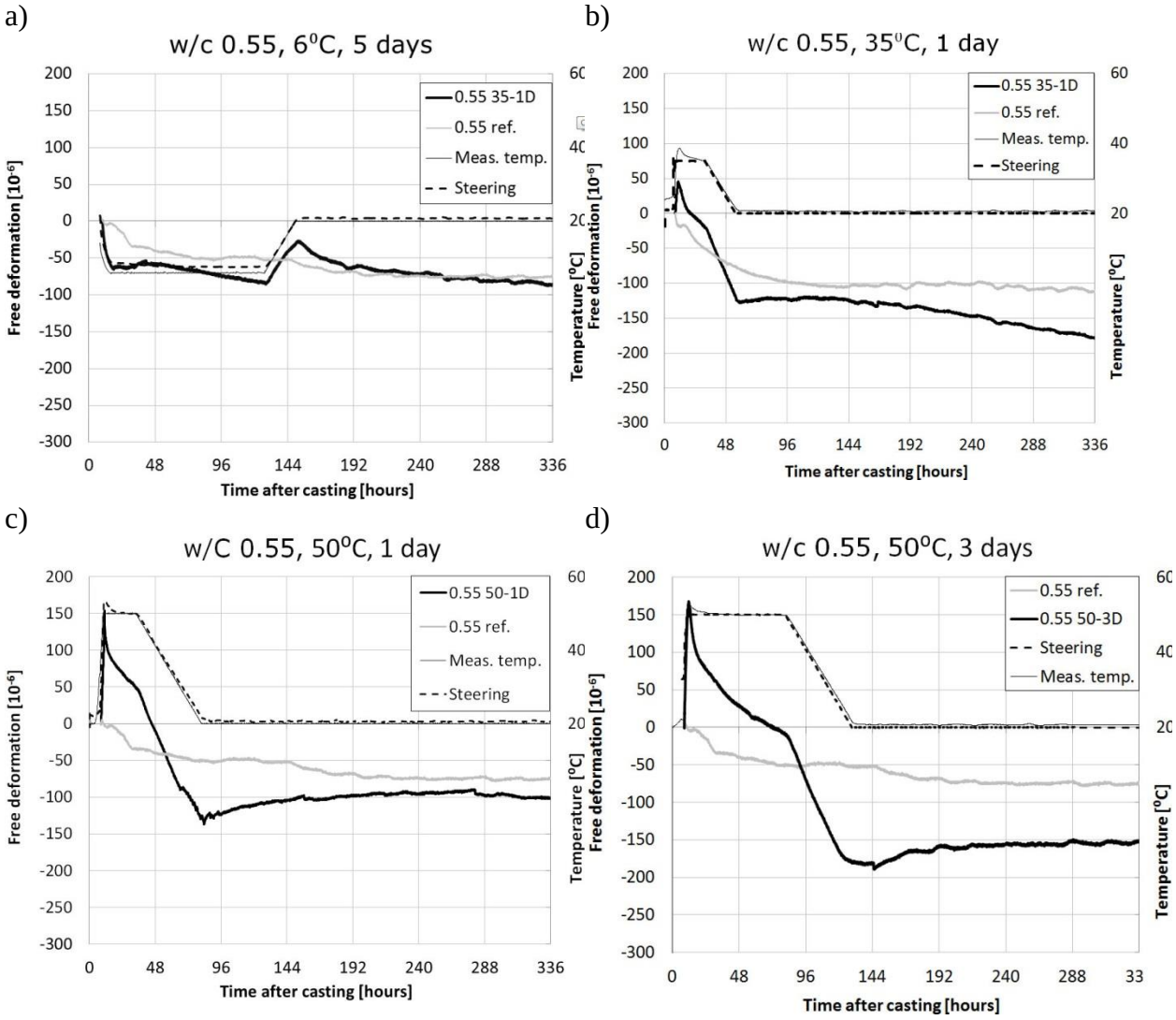

Fig. 6. Individual free deformation plots for w/c 0.55 recipes with BAS cement

A limited study were also done on mixes produced using the ANL cement and ANL cement with flay ash addition (ANLFA). The obtained deformation values are shown in Figure 7. The applied curing regime included application of 50 degrees for 1 and 3 days followed by forced cooling down to 20 degrees. In both cases no pronounced swelling was observed after cooling down as in the case all concretes produced with BAS cement, Figures 5 and 6.

The reasons for the lack of swelling in the case of ANL cements cannot be determined based on the obtained tests results. However, it can be assumed that the cement composition and especially

its tricalcium aluminate content could affect formation of ettringite. The ettringite is known for its expansive potential developing during crystallization (at early age) and re-crystallization (at later ages) processes. Another possible factor is the effects of fly ash and fines of the cement which presumably affected the microstructure and phase composition of hardened binder matrixes.

a) b)

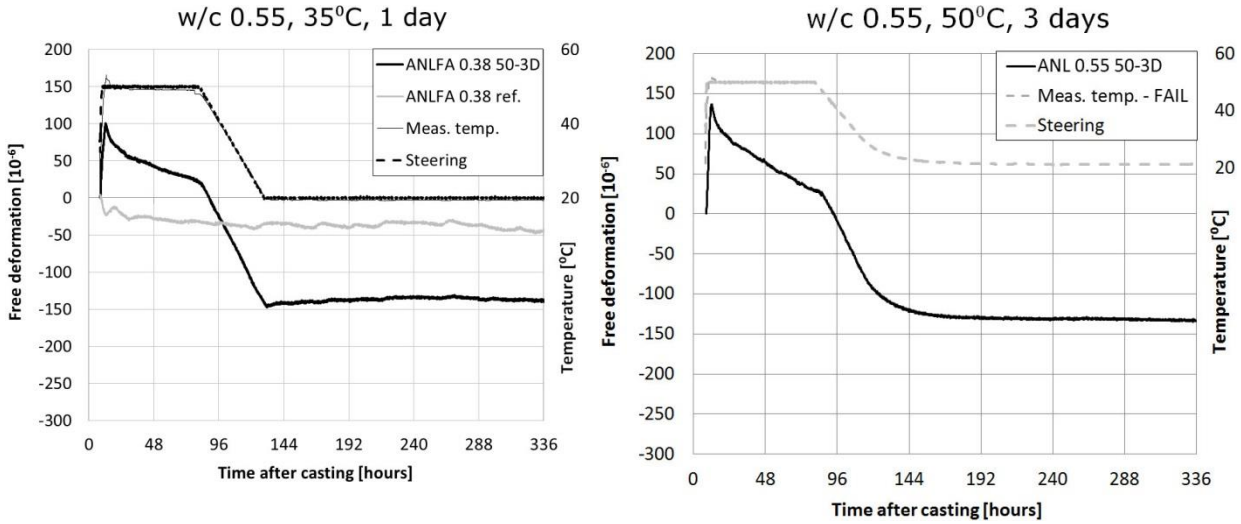

Fig. 7. Individual free deformation plots for w/c 0.55 recipes with ANL cement

5 MODELING

5.1 The HH model (Hans Hedlund, 2000)

The total free movement measured on the concrete sample located in the laboratory room at approximately 20°C is here denoted test *A*, and the test subjected to variable temperature is denoted test *B*. The registered free deformation is the sum of thermal dilation and autogenous shrinkage (Eq. 1).

In the model, fully coupled "total deformation" is calculated, fitted against the measured free deformation through an iterative process. One single, constant thermal expansion coefficient is incorporated both for the heating and for the cooling phase.

The model is based on the maturity concept, i.e., it hinges on the premise that the autogenous shrinkage of a heat-cured sample can be described based on the behavior of a 20°C isothermal reference sample.

It is assumed that it is possible to incorporate the effects of variable temperature curing into a factor $\beta_{ST}(T)$ denoted as "temperature sensitivity factor" or the "temperature effect on autogenous shrinkage". This expression accounts for the temperature in the sample in relation to $T_c^{max}(t)$, the maximum temperature in the sample up to the moment of calculation. It does not, however, account for how long that $T_c^{max}(t)$ – if it is a curing temperature plateau – has been kept. In essence, it accounts for the amplitude of T but not the duration of it, which has shown to be problematic for certain concretes, both in earlier tests at LTU and in the state-of-the-art literature.

Equations used are:

$$\varepsilon_{tot} = \varepsilon_T + \varepsilon_{SH} \tag{1}$$

$$\varepsilon_{SH} = \varepsilon_{ref} \cdot \beta_{s0}(t_e) \cdot \beta_{ST}(T) \tag{2}$$

$$\beta_{s0}(t_e) = \exp\left(-\left[t_{s0}/(t_e - t_{start})\right]^{\eta_{SH}}\right) \tag{3}$$

$$\beta_{ST}(T) = a_0 + a_1 \cdot \left(1 - \exp\left[-T_c^{max}(t)/T_1\right]^{b_1}\right) + a_2 \cdot \left(1 - \exp\left[-T_c^{max}(t)/T_2\right]^{b_2}\right) \tag{4}$$

$$\varepsilon_T = \Delta T_c(t) \cdot \alpha \tag{5}$$

where ε_{tot} [-] = measured strain; ε_T [-] = thermal dilation; ε_{SH} [-] = autogenous shrinkage; ε_{ref} [-] = reference ultimate shrinkage, a fitting parameter decided by the least square method; β_{s0} [-] = relative time development of shrinkage; t_e [s, h or d] = equivalent time of maturity; t_{start} [s, h or d] = start time of autogenous shrinkage specified in real time after mixing; t_{s0} [s, h or d] and η_{SH} [-] = fitting parameters determined by least square method; $\beta_{ST}(T)$ **[-] = temperature sensitivity**

factor; $T_c^{max}(t)$ [°C] = maximum temperature in the concrete sample up to time t; t [s, h or d] = real time specified as time after mixing; a_0 [-], a_1 [-], a_2 [-], b_1 [-], b_2 [-], T_1 [°C], T_2 [°C] = fitting parameters; $\Delta T_c(t)$ [°C] = temperature difference in the concrete sample; T_{max} [°C] = maximum measured temperature for the concrete sample; α [°C^{-1}] = thermal expansion/contraction coefficient.

General fitting parameters have been evaluated by Hedlund (2000), and proposed as shown in Table 4 for NSC and HSC.

Table 4. Evaluated fitting parameters by (Hedlund, 2000)

Type of concrete	a_0 [-]	a_1 [-]	T_1 [°C]	b_1 [-]	a_2 [-]	T_2 [°C]	b_2 [-]
NSC	0.4	0.6	9	2.9	1.3	55	7
HSC	0.4	0.6	9	2.9	0.1	55	7

5.2 Using the HH model

The iteration can be run optimized for Sample B, or for both the 20^0C reference (A) and the heat-cured sample (B) at the same time.

All deformation values have been zeroed at first setting time, at 8.5 hours after casting. The timescales have been converted to equivalent time for direct comparison.

It is important to note that the duration of the tests has been 14 days – based on earlier tests at LTU this was assumed to be sufficiently long for the shrinkage to stabilize. However, with the expansion measured, it turned out to be insufficient because the expansion did not level off during this time. This means that the entire modeling is done, effectively, on **cropped data**.

5.3 Results

5.3.1 Evaluated fitting parameters

Tables 5 and 6 contain the evaluated fitting parameters for the best fit, determined by the least square method. All fitting is optimized for Sample B (heat-cured).

Table 5. Fitting parameters

Recipe	Curing	θ_{ref} [K]	κ_3 [-]	t_{s0} [h]	t_{start} [h]	ε_{ref} [10^{-6}]	η_{SH} [-]	α_T [$10^{-6}/^0$C]
BAS1	all	3150	0.275	8.5				
	6-5D				30	-290	1.5	10
	35-1D				60	-42	0.6	9.8
	50-1D				8.5	-170	1	9.9
	50-3D				9.9	-52	1.1	11.1
BAS2	all	3150	0.275	8.5				
	6-5D				60	-139	0.4	9.5
	35-1D				60	-186	0.2	10.1
	50-1D				60	-156	3.8	9.3
	50-3D				60	-120	5	11.5

Table 6. Fitting parameters

Recipe	Curing	a_0 [-]	a_1 [-]	T_1 [°C]	b_1 [-]	a_2 [-]	T_2 [°C]	b_2 [-]
BAS1	6-5D	0.1	0.5	9	2.9	0.1	55	7
	35-1D	2.2	1.9	9	2.9	0.9	55	6.5
	50-1D	2.0	-1.3	9	2.9	2.6	73	9.2
	50-3D	1	1.3	9	2.9	0.5	55	6.9
BAS2	6-5D	1.2	0.1	9	2.5	1.9	55	5.8
	35-1D	-2.2	1.4	9	3.4	3.9	55	6.0
	50-1D	-1.0	1.0	9	5.3	1.2	50	5.0
	50-3D	0.2	0.2	9	0.2	0.7	55	7.0

Only individual evaluation – for each separate test, per concrete and temperature level – has been carried out. The fitting parameters differ substantially so that mass-fitting (across all tests for the same recipe) does not appear to be feasible at the moment.

In general, it can be said that the fitting parameters appear to be unsystematic. The calculated ε_{ref} values are more uniform for the BAS2 concrete. The BAS1 concrete shows a much larger scatter. Sometimes, a_0 and a_1 get negative values for best fitting, in a non-systematic way.

5.3.2 Individual fitting; plots

Full results are found in Appendix 1.

Only a couple of representative plots are shown here.

"Free def. meas." denotes the lab measured coupled deformation. "Free def. calc." is the best fitting achieved by the HH model through the least square fitting. AD and TD are autogenous and thermal deformations, respectively.

Figure 8 illustrates that, for the same concrete, otherwise identically behaving reference samples (in terms of free measurement) cannot be modeled well when the calculation is optimized for the prescribed sample. AD is overestimated in Figure 8a, while acceptable in terms of end value, but overestimated early on, in Figure 8b.

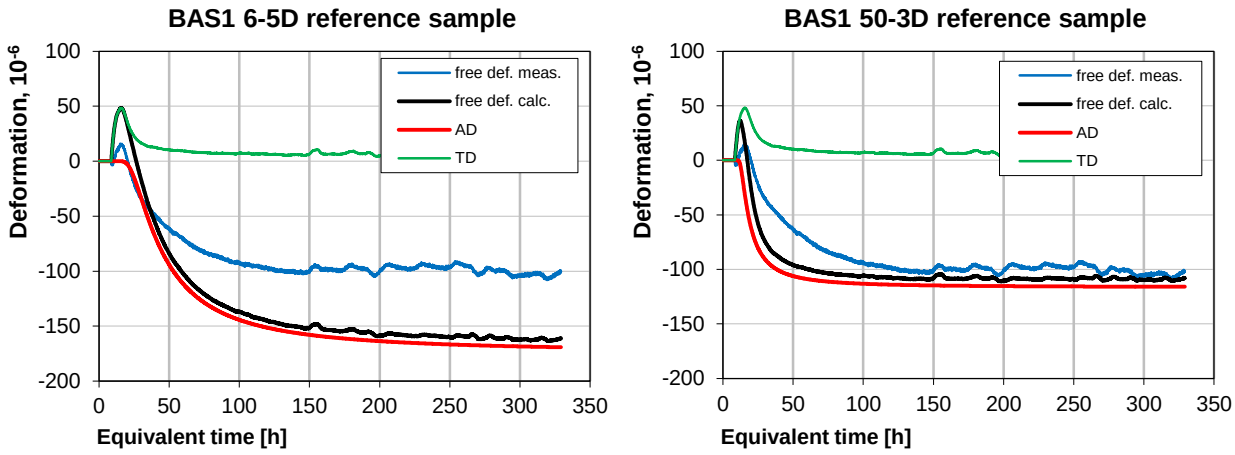

Fig. 8. Worst case fitting for reference samples in BAS1 concrete

The overall worst fit is for both cooled down samples. One of them, the BAS1 concrete is plotted in Figure 9. For some reason, the AS develops at a very fast rate early on, up to about 24 hours after casting – in equivalent time, which cannot be modeled satisfactorily. The heating up phase is modeled adequately, but not the stage at which the temperature stabilizes at room temperature again. Moreover, it can be clearly seen that the TD part is not calculated as a flat line when the temperatures are kept constant.

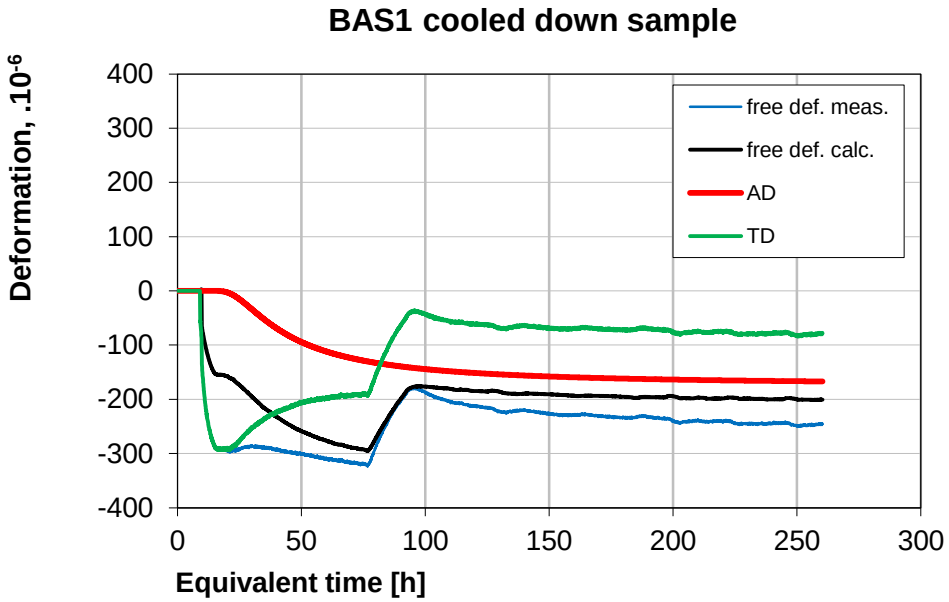

Fig. 9. Behavior of the cooled down samples

The typical behavior for the heated samples is illustrated in Figure 10. The initial peak due to heat of hydration is slightly overestimated by the model. Neither during the heat-curing plateau nor the cooling down phase is modeled precisely, but the main issue with the model, nonetheless, is when the total deformation indicated expansion. The HH model can only calculate scratch shrinkage for AD, and offset the total deformation with that to calculate TD. The TD calculated should be a flat line after 150 hours, considering that the temperature is constant, but instead the sample appears to be being heated up.

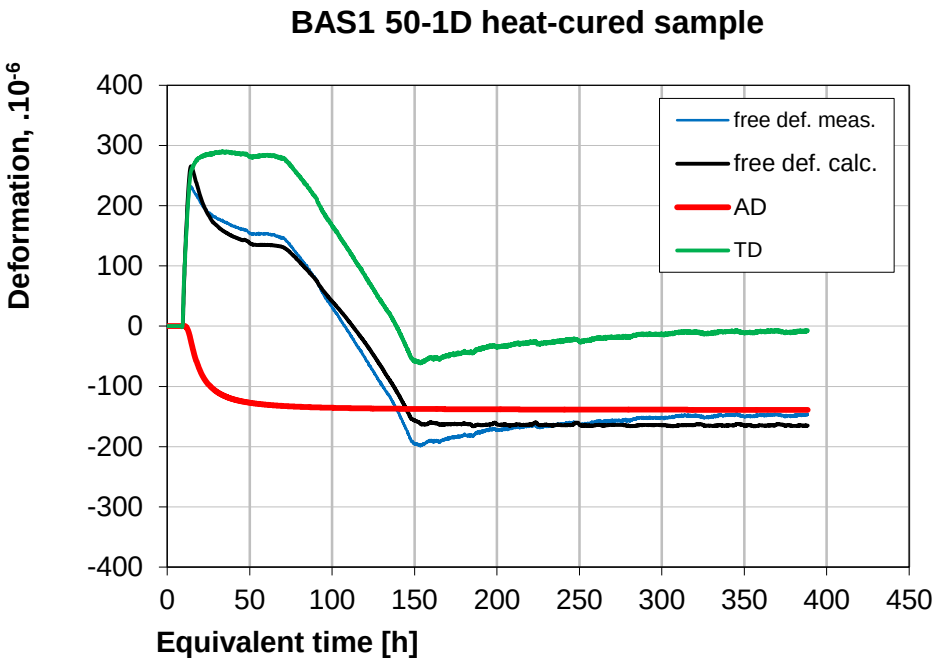

Fig. 10. Typical behavior of heated samples

5.4 Discussion of results – Validity of the HH model

Fit for the reference samples are unacceptable; in particular for the 35^{0}C temperature level (both recipes) and the 50^{0}C levels for BAS2.

As it can be seen in all heat-cured samples, even in the case of best fitting, AD swelling cannot be accommodated. For AD, strictly contraction can be calculated only due to the fact that the total deformation is calculated as a function of the shrinkage of the 20^{0}C reference (i.e., applying the maturity concept), which is a monotonic decreasing function.

Contraction is calculated even where expansion has been measured at constant temperatures. As a consequence, TD is also calculated incorrectly; since it is calculated back from the incorrectly fitted total deformation. TD should be constant where the curing temperature is kept constant (during curing plateau/after the cooling down phase), but the calculated TD $\varepsilon_T = \varepsilon_{tot} - \varepsilon_{SH}$ mimics a sample being warmed up.

Another apparent inconsistency the model reveals is that autogenous shrinkage in the heat-cured samples is calculated to be identical or even less than AS of the 20°C isothermal references, effectively saying that the curing temperature has no effect on AD and that the larger free deformations are measured purely due to TD.

5.5 Constant coefficient splitting – a phenomenological investigation

As it has been shown, both AD and TD in the HH model are calculated incorrectly. It is certain that where the temperature is constant (i.e., TD = 0), if the free deformation indicates expansion, it *must be due to AD*. The model relates AD to the AD of the isothermal reference, therefore it is unable to account for expansion.

In an attempt to have a better understanding of the nature (*realistic* shape) of AD under variable temperature levels (vs. 20^0C isothermal tests), and to see how the assumption of TD affects the AD, manual splitting of total deformation into AD and TD has been performed, assuming various (however, still constant) CTEs ranging from $8x10^{-6}$ $1/^0$C to $12x10^{-6}$ $1/^0$C, based on literature for mature concrete. In this approach, instead of making assumptions of how the AD of a heat-cured sample can or cannot be related to the AD (strict *contraction*) of a reference sample, an assumption of the TD is made. Ideally, TD(t) would be determined in the lab.

Only example of the splitting is presented here in Figure 10. The rest of the figures can be found in Appendix 2.

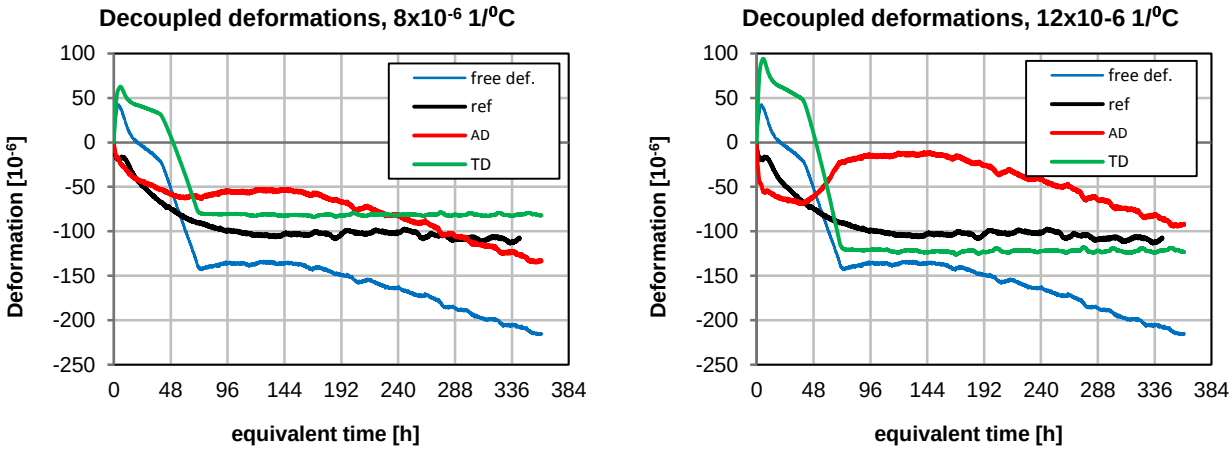

Fig. 10. Calculated development of thermally influenced AD at variable curing temperatures in BAS1, cured at 35 degrees for 1 day. Ref – 20^0C isothermal reference

5.5.1 Discussion

The individual plots reveal that, regardless of the choice of CTE, the deduced *AD will be morphologically different* from that of the 20^0C isothermal reference. All individual AD plots exhibit a certain amount of swelling, regardless of temperature level – hence, the AD of heat cured samples is morphologically different from the reference sample. This suggests that it is not possible to model the AD development under variable temperatures based on the behavior of the 20^0C isothermal sample. This conclusion is in line with the findings of several researchers, as presented in 1.2, Decoupling autogenous and thermal deformation.

Similarly to the HH model, the manual splitting reveals that the initial expansion at the onset of the heat curing is due to purely thermal expansion (due to heat of hydration). Beginning at the onset of the cooling down phase, a marked swelling can be observed which continues throughout the entire cooling down phase and, depending on temperature level, it may not level off during the entire 14-day duration of the tests.

Furthermore, it can be seen that varying the CTE results in a set of AD and TD curves, *mostly* parallel to each other. However, the onset, and the rate of the swelling also change. By choosing a lower CTE ($8x10^{-6}$ $1/^0$C) results in minimal swelling, while a higher CTE ($12x10^{-6}$ $1/^0$C) will result in a very distinct swelling at a fast rate. The next plot is a comparison between the lowest and the

highest CTE to show how the onset of the swelling changes; *higher CTE will bring the onset of the swelling forward* in time; see the onset of swelling at around 230 hours for the lowest, and at 168 hours for the highest CTE chosen – the difference is nearly three days.

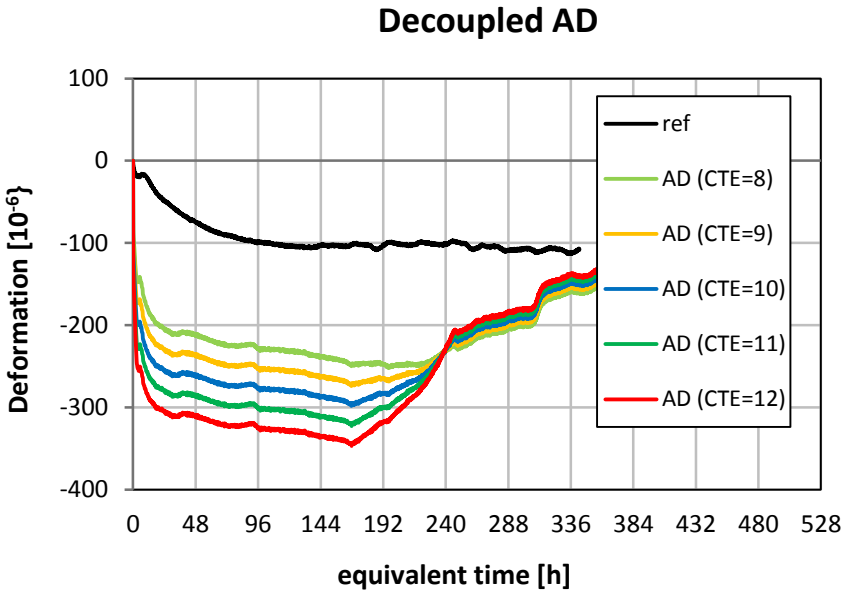

Fig. 11. Effects of choice of CTE

The results underline the importance of experimentally determining the correct CTE(t), without which no correct AD can be calculated (or modeled).

5.5.2 Comparative analysis, BAS1 w/c 0.38

Unsystematic behavior is revealed when plotting all AD curves against the reference sample, in terms of equivalent time in Figure 12, similarly to that presented in [10] and [16].

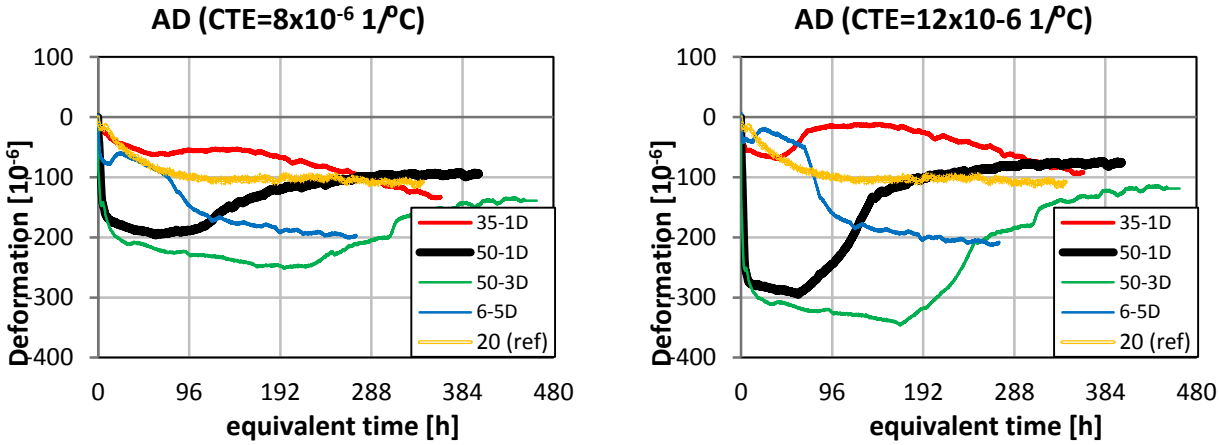

Fig.12. Unsystematic AD behavior regardless of choice of CTE.

The magnitude of the AD, naturally, varies with on the choice of the CTE. The character of the curves does not change as substantially – where there has been swelling with a lower CTE, there

is swelling with a higher CTE as well – but the onset of the swelling does vary. Higher CTE corresponds to earlier onset of swelling.

The 35^{0}C sample will shrink less than the 20^{0}C isothermal sample up to a certain point (288…336 hours in terms of equivalent time, depending on CTE) when a crossover effect is observed as the 35^{0}C sample turns into shrinkage again and shrinks at a faster rate than the 20^{0}C reference. Both 50^{0}C samples begin to shrink at a higher rate than any other temperature levels. However, they exhibit a long lasting expansion that does not level off completely during the 2 weeks the tests were running. It is expected that the expansion would eventually turn into contraction again. The 6^{0}C sample behaves in a unique way. A very early onset swelling appears to be related to the rapid cooling down is followed by a contraction happening at a faster rate than the 20^{0}C isothermal sample. It is commonly accepted that lower temperatures would hinder shrinkage rather than accelerate it.

5.5.3 Comparative analysis, BAS2 w/c 0.55

A similar phenomenological investigation has been carried out for the second BAS recipe. Without details, the summary is shown in Figure 13. All plots can be found in Appendix 3.

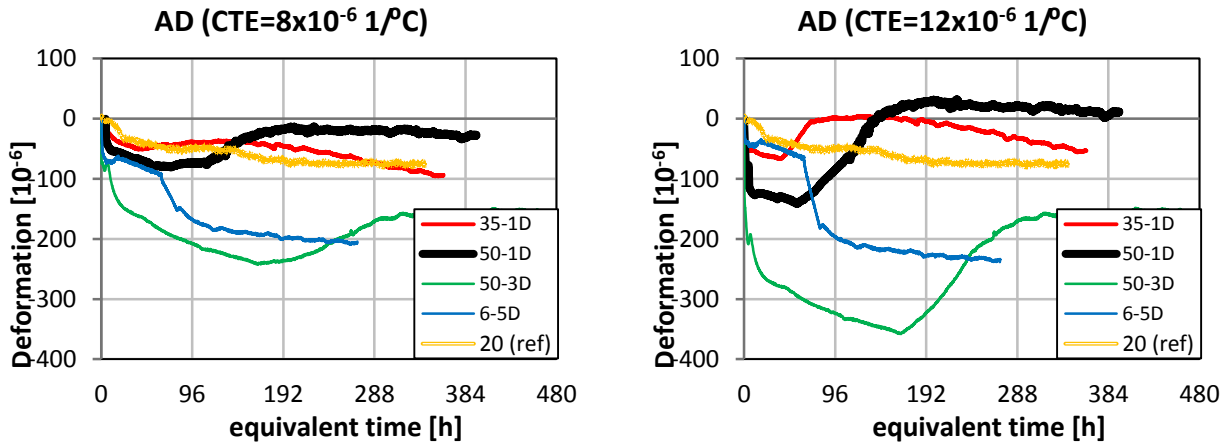

Fig.13. Unsystematic AD behavior regardless of choice of CTE.

All conclusions for the BAS1 w/c 0.38 recipe are still valid here regarding the unsystematic behavior (crossover effect between 20^{0}C and 35^{0}C sample, swelling, etc.).

The 20^{0}C and 35^{0}C samples shrink marginally less than the w/c 0.38 samples for the same curing temperature.

The difference between the 50-1D and the 50-3D samples is much more prominent. The 50-1D exhibits substantially smaller early deformations the 3D counterpart, which is suspicious considering that the behavior should be identical until 1 day into the heat curing. This could be due to “user error”, as the 50-1D mix was the earliest test run while both the mixing & testing routine and the equipment were still not perfected.

6 CONCLUSIONS

Based on the results of this study the following conclusions can be formulated:

Phenomenological point of view

- Heat curing at variable temperature levels induces non-negligible autogenous swelling that may mitigate some of the stresses arising from shrinkage when the concrete is very young.
- The higher the curing temperature and the longer the duration of heat curing, the more prominent was the swelling, in particular for the low w/c mix.
- Lower curing temperatures (35°C) have not resulted in significantly smaller swelling.
- Cement type, especially its fines and tricalcium aluminate content, may be contributing factors affecting the extent of the autogenous swelling. The presence and type of fly ash could be presumably another contributing factor to the extent of autogenous swelling (based on literature).
- In the very limited testing, the swelling could not be traced back directly to the FA content of the cement (BAS) vs. ANL (no FA). The ANLFA "home" mix with 30% FA exhibited no noticeable swelling.
- Cold curing (6ºC) which simulated cold weather casting has shown to delay, but not to mitigate the ultimate deformation.
- The observed expansion did not level off during the 2-week duration of the testing. Originally, the set-up and steering had been designed to provide input data for adapting existing autogenous shrinkage models to variable curing temperatures. The autogenous swelling, at the stage of planning, was not expected in these recipes/tests. Therefore, the evaluation based on both the HH model and the phenomenological investigation of AD-TD has been done on "cropped" data. The final (design) value of AD cannot be predicted.

Modeling

- The HH model would give an acceptable fit for some of the reference samples, but a bad fit for all heat-cured samples after the cooling down stage, and a few reference samples as well, in an inconsistent way.
- The HH model likely underestimates the end value of AD because (1) of the cropped data and (2) for several evaluated tests, there is no significant difference between the AD of the reference sample and that of the heat-cured sample.
- The thermal dilation part is visibly wrong.
- AD is always modeled as contraction. The HH model is not able to accommodate AD swelling.
- Due to limited resources, the development of CTE over time has not been calibrated in this study. This is a major limitation as the highly nonlinear nature of CTE in young concrete is well-known and therefore, splitting of the free deformation into AD and TD is not possible without an accurate CTE(t). If an incorrect CTE is used at any stage, it is possible

that back-calculated “AD swelling” may be partly or entirely from thermal origin. While CTE itself has not been the focus of the study, the nonlinearity in free deformations observed during the cooling off stages of the imposed temperature paths have supported evidence to the highly nonlinear nature of CTE in young concrete.

7 RECOMMENDATIONS REGARDING PRODUCTION, EXECUTION ASPECTS AND IMPROVED QUALITY

The study showed that existing models have certain drawbacks mostly related to a possible swelling which is not accounted for. That phenomenon becomes increasingly important for new generation of composite Portland cements and when secondary cementitious binders are used.

The results obtained within this project have clarified problems of current models and as such it is an excellent foundation for more detailed future research leading to the development of new more reliable models. One new aspect which should be studied in depth is a possibility to utilize the observed swelling to decrease cracking risk of young concrete. If that swelling would be introduced in a controlled manner for example by a proper concrete mix design or optimized curing it could decrease shrinkage and thus cracking risk of young concretes when the tensile strength is relatively low.

Successful implementation of that approach would lead to development of improved "crack free" concrete. It would alter the production processes, concreting technology and would improve quality of hardened concrete. Lower crack risk would also enhance the sustainability of that material and decrease early age repair costs.

8 ACKNOWLEDGEMENTS

The funding for this project was provided by Trafikverket (Swedish Road Administration) and SBUF (Development Fund of the Swedish Construction Industry). The materials were supplied by Cementa Ltd., Sweden. Their support is greatly appreciated along with the technical help from the lab staff at LTU. Furthermore, Prof. Jan-Erik Jonasson is greatly acknowledged for his support in planning the experimental program.

9 REFERENCES

[1] P. Lura, Autogenous deformation and internal curing of concrete, Doctoral Thesis, Delft University of Technology, the Netherlands, 2003.

[2] B. Persson, Self-desiccation and its importance in concrete technology, Materials and Structures. 30 (1997) 293–305.

[3] O.M. Jensen, P.F. Hansen, Autogenous deformation and RH-change in perspective, Cement and Concrete Research. 31 (2001) 1859–1865.

[4] E. Tazawa, R. Sato, E. Sakai, S. Miyazawa, Work of JCI committee on autogenous shrinkage, in: Proc. Shrinkage 2000-Int. RILEM Workshop on Shrinkage of Concrete, 2000: pp. 21–40.

[5] O.M. Jensen, P.F. Hansen, Influence of temperature on autogenous deformation and relative humidity change in hardening cement paste, Cement and Concrete Research. 29 (1999) 567–575.

[6] P. Lura, O.M. Jensen, K. van Breugel, Autogenous shrinkage in high-performance cement paste: an evaluation of basic mechanisms, Cement and Concrete Research. 33 (2003) 223–232.

[7] E.E. Holt, Early age autogenous shrinkage of concrete, Technical Research Centre of Finland (VTT), 2001.

[8] K. Kovler, S. Zhutovsky, Overview and future trends of shrinkage research, Materials and Structures. 39 (2006) 827–847.

[9] D. Cusson, T. Hoogeveen, Internal curing of high-performance concrete with pre-soaked fine lightweight aggregate for prevention of autogenous shrinkage cracking, Cement and Concrete Research. 38 (2008) 757–765.

[10] Ø. Bjøntegaard, Thermal Dilation and Autogenous Deformation as Driving Forces to Self-Induced Stresses in High Performance Concrete, The Norwegian University of Science and Technology, 1999.

[11] H. Hedlund, J.-E. Jonasson, Effect on stress development of restrained thermal and moisture deformation, Proceedings of Shrinkage. (2000) 355–375.

[12] P. Turcry, A. Loukili, L. Barcelo, J.M. Casabonne, Can the maturity concept be used to separate the autogenous shrinkage and thermal deformation of a cement paste at early age?, Cement and Concrete Research. 32 (2002) 1443–1450.

[13] M. Emborg, Thermal stresses in concrete structures at early age, Doctoral Thesis, Luleå University of Technology, 1989.

[14] H. Hedlund, Hardening Concrete: Measurements and Evaluation of Non-Elastic Deformation and Associated Restraint Stresses, Doctoral Thesis, Luleå University of Technology, 2000.

[15] Ø. Bjøntegaard, E.J. Sellevold, Interaction between thermal dilation and autogenous deformation in high performance concrete, Materials and Structures. 34 (2001) 266–272.

[16] A.B. Klausen, Early age crack assessment of concrete structures: Experimental investigation of decisive parameters, 2016.

[17] P. Lura, K. van Breugel, I. Maruyama, Effect of curing temperature and type of cement on early-age shrinkage of high-performance concrete, Cement and Concrete Research. 31 (2001) 1867–1872.

[18] I. Chu, S.H. Kwon, M.N. Amin, J.-K. Kim, Estimation of temperature effects on autogenous shrinkage of concrete by a new prediction model, Construction and Building Materials. 35 (2012) 171–182.

[19] F. Grondin, M. Bouasker, P. Mounanga, A. Khelidj, A. Perronnet, Physico-chemical deformations of solidifying cementitious systems: multiscale modelling, Materials and Structures. 43 (2010) 151–165.

[20] E. Sellevold, O. Bjøntegaard, Coefficient of thermal expansion of cement paste and concrete: mechanisms of moisture interaction, Materials and Structures. 39 (2006) 809–815.

[21] M. Viviani, B. Glisic, I.F.C. Smith, Separation of thermal and autogenous deformation at varying temperatures using optical fiber sensors, Cement and Concrete Composites. 29 (2007) 435–447.

[22] Z.C. Grasley, D.A. Lange, Thermal dilation and internal relative humidity of hardened cement paste, Materials and Structures. 40 (2007) 311–317.

[23] D. Cusson, T. Hoogeveen, Measuring early-age coefficient of thermal expansion in high-performance concrete, in: International RILEM Conference on Volume Changes of Hardening Concrete: Testing and Mitigation. RILEM Publication, Lyngby, Denmark, 2006.

[24] R. Loser, B. Münch, P. Lura, A volumetric technique for measuring the coefficient of thermal expansion of hardening cement paste and mortar, Cement and Concrete Research. 40 (2010) 1138–1147.

[25] A. Loukili, D. Chopin, A. Khelidj, J.-Y. Le Touzo, A new approach to determine autogenous shrinkage of mortar at an early age considering temperature history, Cement and Concrete Research. 30 (2000) 915–922.

[26] I. Maruyama, A. Teramoto, Temperature dependence of autogenous shrinkage of silica fume cement pastes with a very low water–binder ratio, Cement and Concrete Research. 50 (2013) 41–50.

[27] E.J.. Sellevold, Ø. Bjøntegaard, T.A. Hammer, Response to discussion of the paper:"On the measurement of free deformation of early age cement paste and concrete"[Bjøntegaard Ø, Hammer TA, Sellevold EJ. Cement and Concrete Composites 2004; 26: 427-435], Cement and Concrete Composites. 27 (2005) 857–858.

[28] P. Termkhajornkit, T. Nawa, M. Nakai, T. Saito, Effect of fly ash on autogenous shrinkage, Cement and Concrete Research. 35 (2005) 473–482.

[29] I. Maruyama, A. Teramoto, Impact of time-dependent thermal expansion coefficient on the early-age volume changes in cement pastes, Cement and Concrete Research. 41 (2011) 380–391.

[30] D.P. Bentz, O.M. Jensen, K.K. Hansen, J.F. Olesen, H. Stang, C.-J. Haecker, Influence of Cement Particle-Size Distribution on Early Age Autogenous Strains and Stresses in Cement-Based Materials, Journal of the American Ceramic Society. 84 (2001) 129–135.

[31] P. Fjellström, Measurement and Modelling of Young Concrete Properties, Licentiate Thesis, Luleå University of Technology, 2013.

[32] K. Orosz, P. Fjellström, J-E. Jonasson, M. Emborg, H. Hedlund, Evaluation of thermal dilation and autogenous shrinkage at sealed conditions, XXII Nordic Concrete Research Symposium, Iceland, 2014.

10 APPENDIX 1

HH model, individual fittings

BAS 1 concrete cured at 6, 35, and 50 degrees

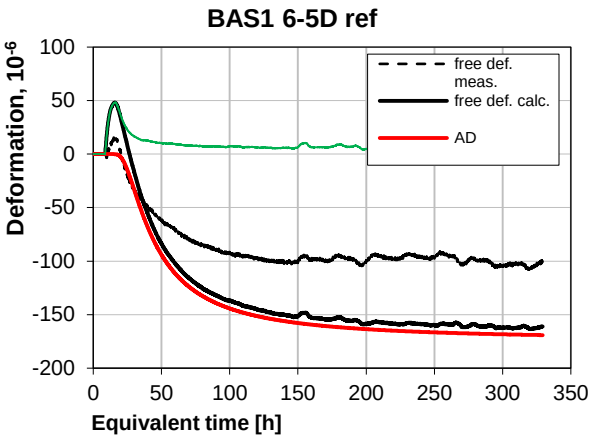

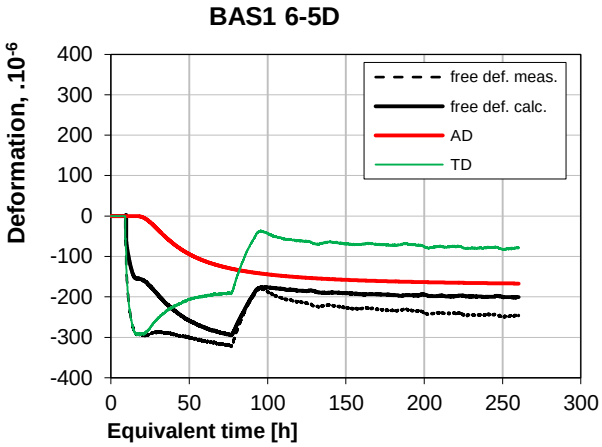

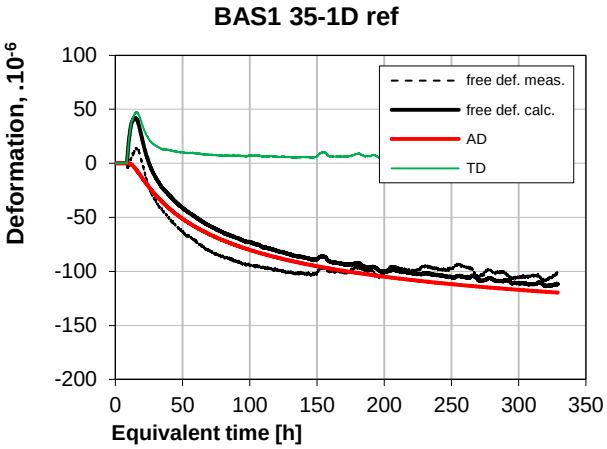

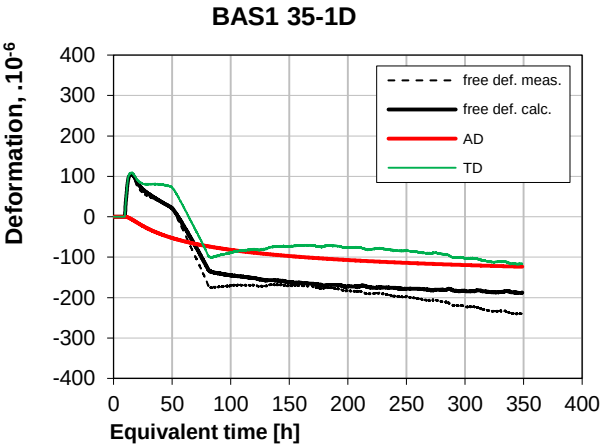

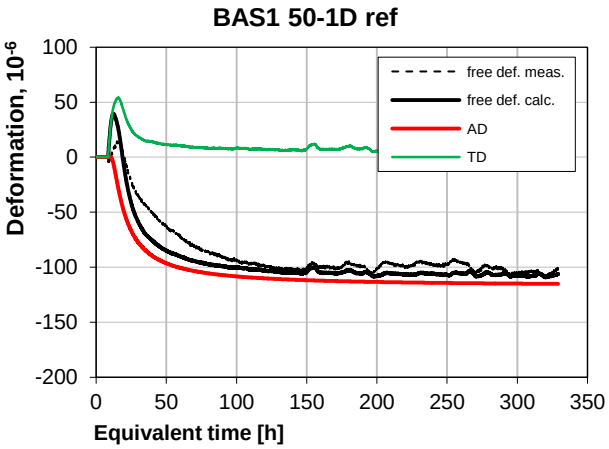

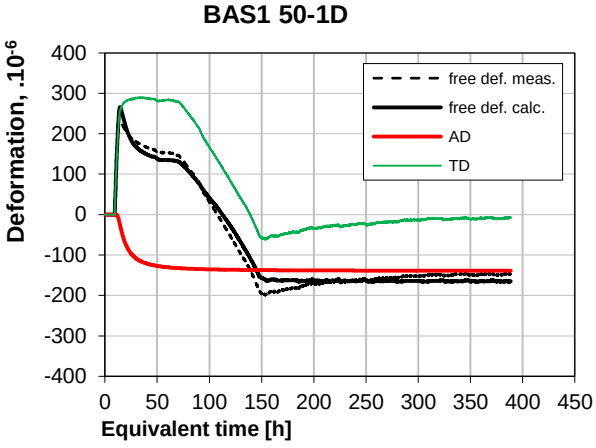

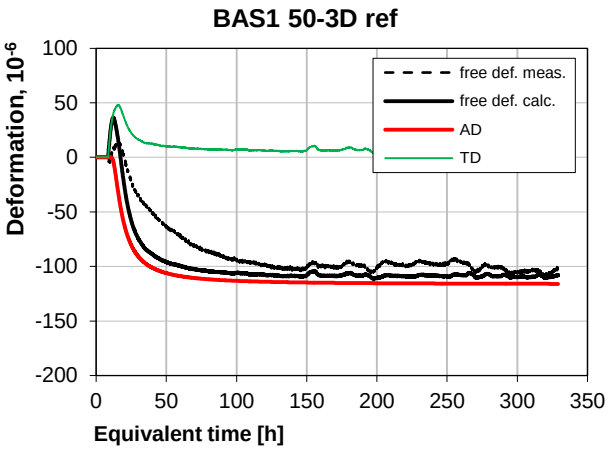

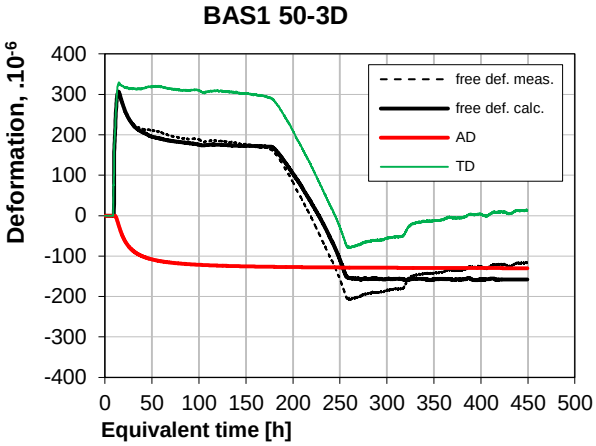

BAS2 concrete cured at 6, 35, and 50 degrees

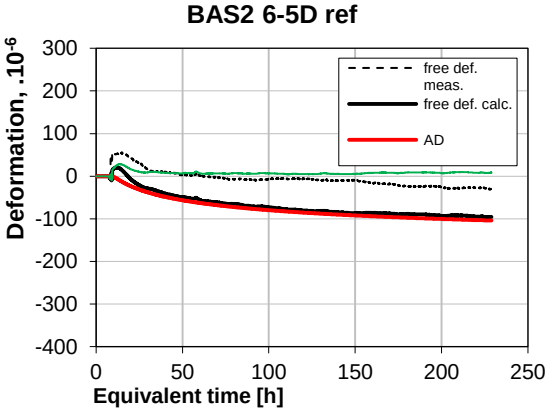

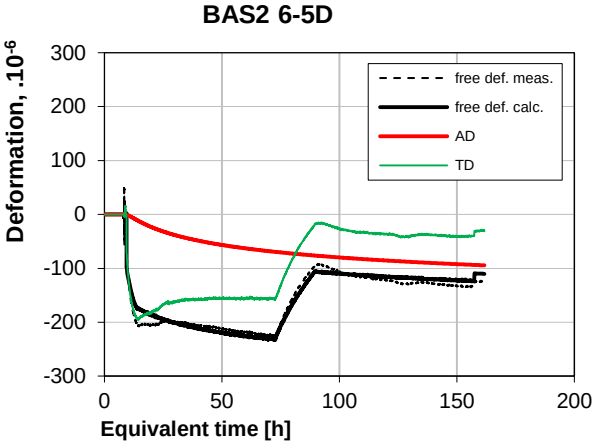

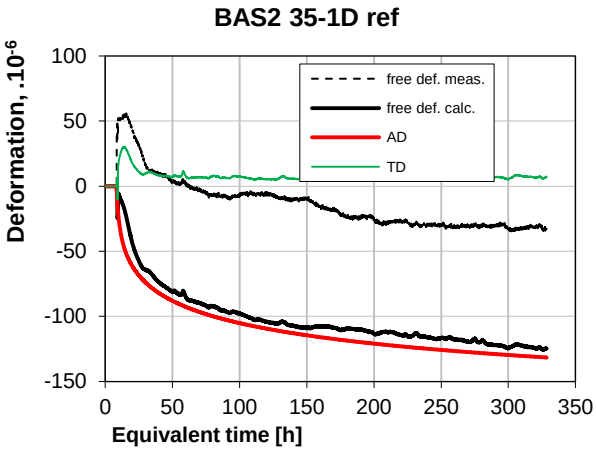

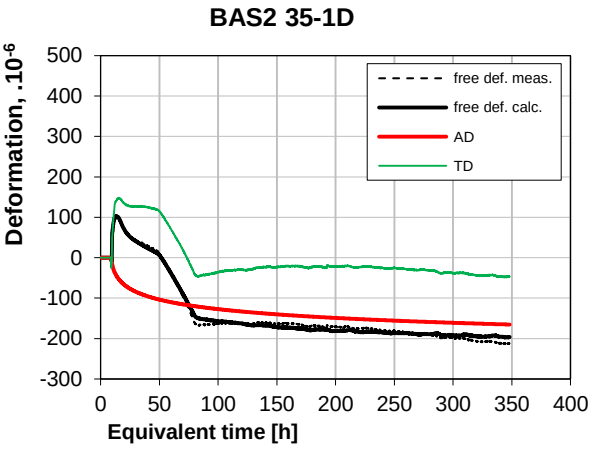

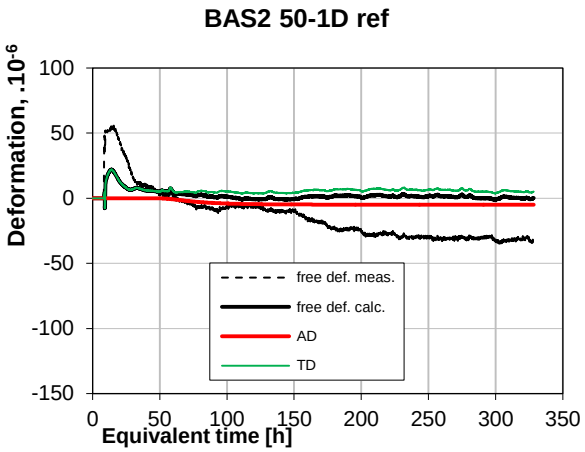
BAS2 50-1D ref
Deformation, .10-6
Equivalent time [h]
free def. meas.
free def. calc.
AD
TD

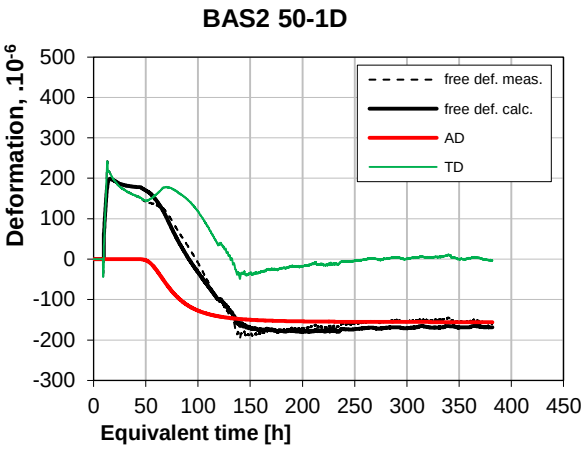
BAS2 50-1D
Deformation, .10-6
Equivalent time [h]
free def. meas.
free def. calc.
AD
TD

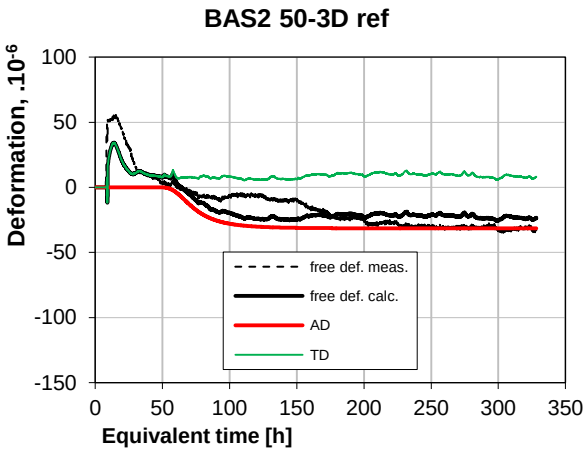
BAS2 50-3D ref
Deformation, .10-6
Equivalent time [h]
free def. meas.
free def. calc.
AD
TD

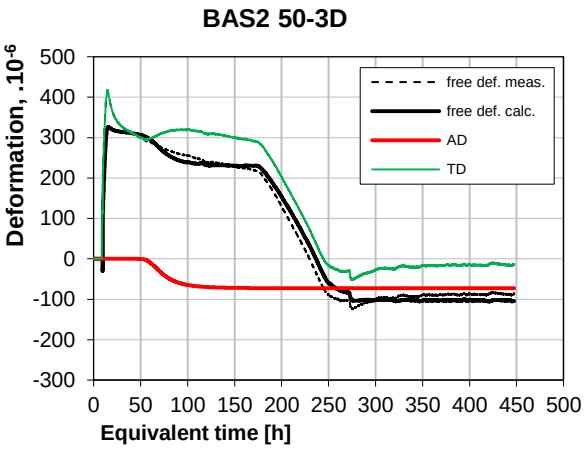
BAS2 50-3D
Deformation, .10-6
Equivalent time [h]
free def. meas.
free def. calc.
AD
TD

11 APPENDIX 2

Constant coefficient splitting – a phenomenological investigation

For the first chosen recipe/temperature level, five individual plots show AD and TD for each chosen CTE (8, 9, 10, 11, and 12 x 10^{-6} $1/^{0}C$) and a final, sixth plot shows the effects of the highest and lowest chosen CTE (the two extreme cases). For all other temperature levels, only the extremes are shown.

Decoupled deformations for BAS1, w/c 0.38

Temperature level 35-1D

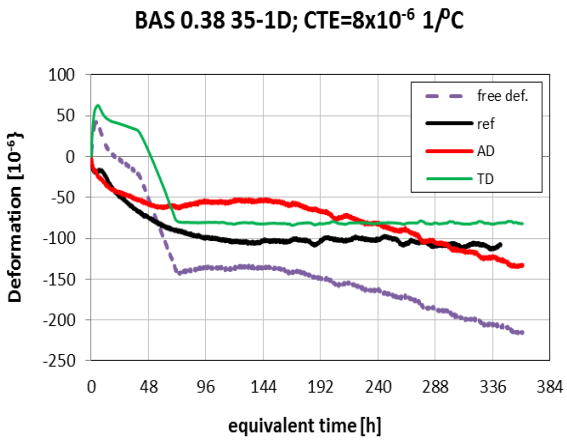

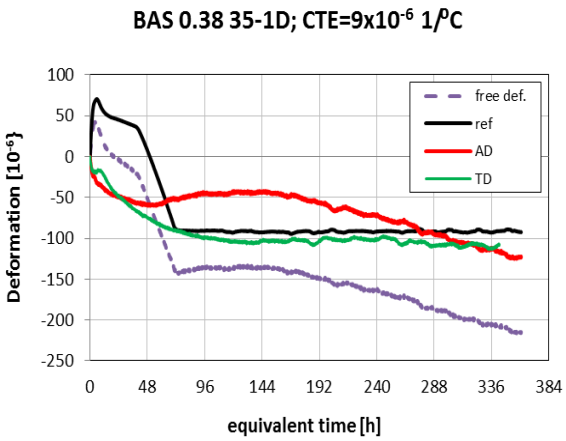

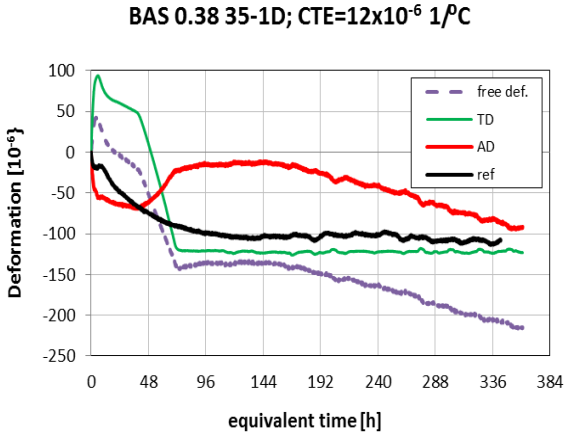

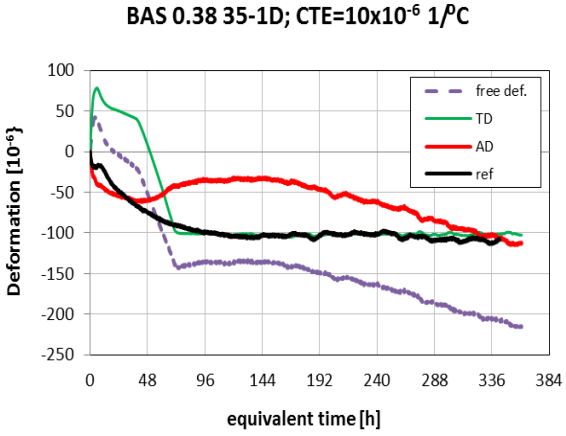

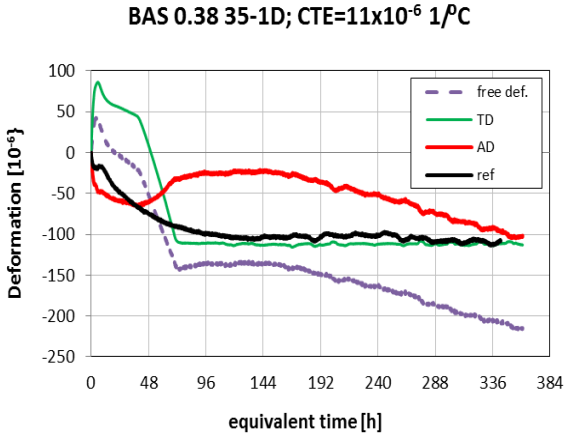

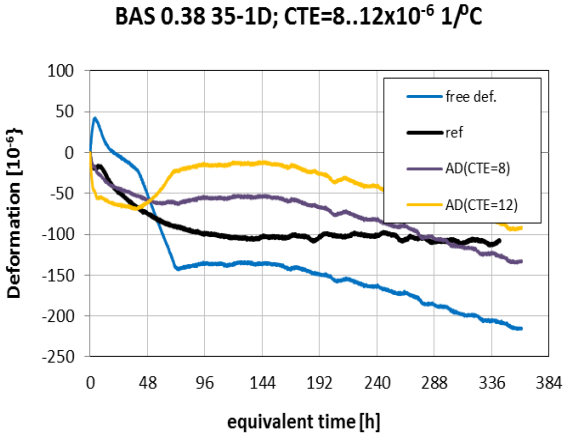

All temperature levels

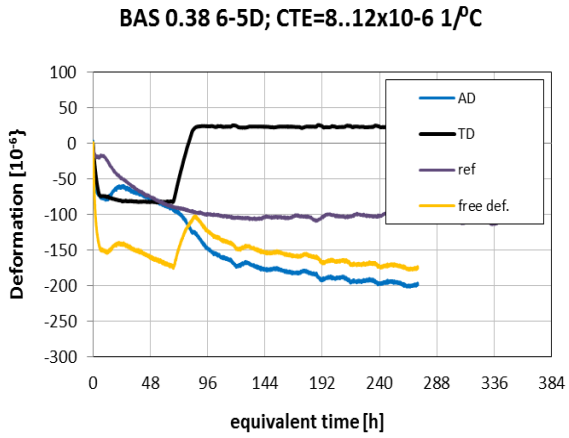

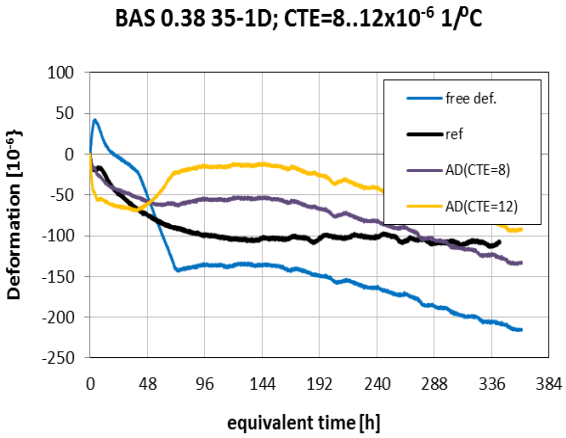

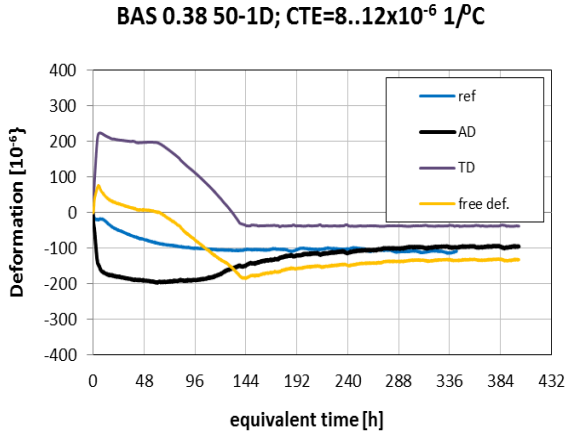

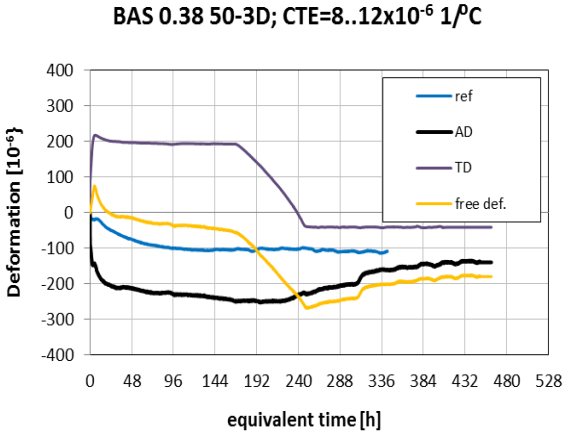

Decoupled deformations for BAS2, w/c 0.55, all temperature levels

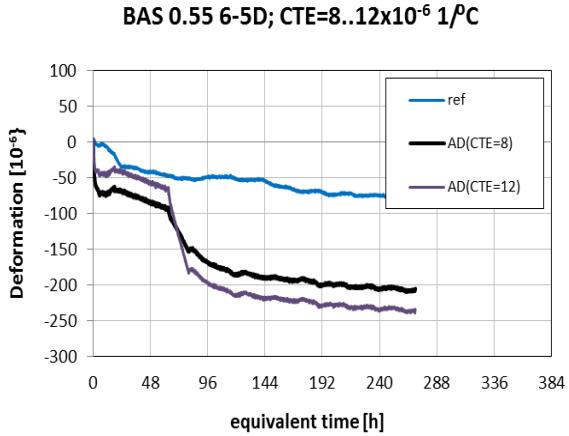

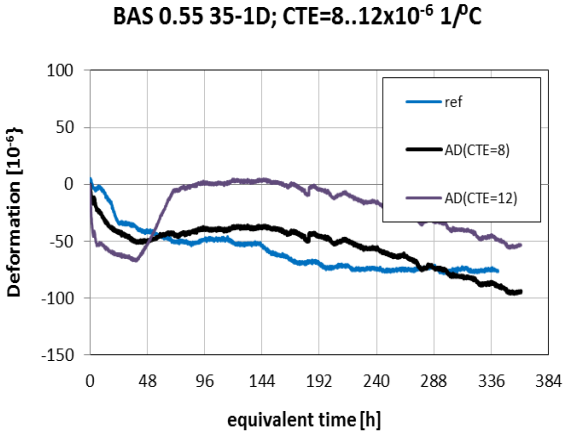

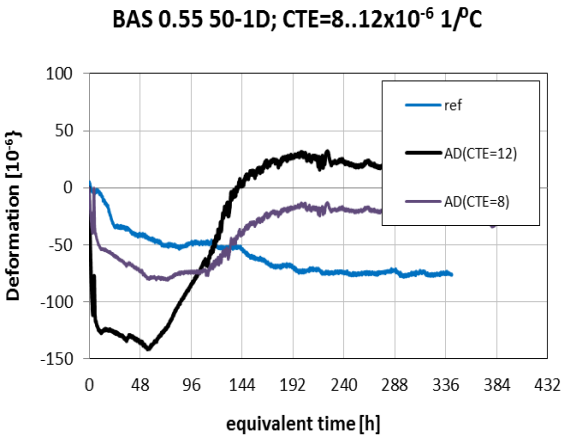
BAS 0.55 50-1D; CTE=8..12x10-6 1/°C
Deformation [10-6]
100
50
0
-50
-100
-150
0
48
96
144
192
240
288
336
384
432
equivalent time [h]
ref
AD(CTE=12)
AD(CTE=8)

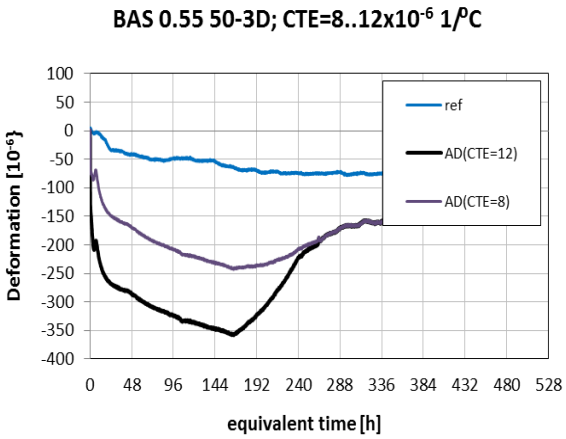
BAS 0.55 50-3D; CTE=8..12x10-6 1/°C
Deformation [10-6]
100
50
0
-50
-100
-150
-200
-250
-300
-350
-400
0
48
96
144
192
240
288
336
384
432
480
528
equivalent time [h]
ref
AD(CTE=12)
AD(CTE=8)